

Authors: Stefanie Kaboth, Patrick Grunert and Lucas J. Lourens  
Title: Mediterranean outflow Water variability during the Early Pleistocene  
Journal: Climate of the Past

Corresponding author's E-Mail address: stefaniekaboth@ntu.edu.tw

Dear Editor,

Firstly, we would like to thank our two anonymous Referees for their careful handling of the manuscript as well as for the constructive comments and suggestions which we kindly acknowledge.

The main criticism of the two referees generally concentrated on: (1) the validity of the grain-size distribution and its corresponding spectral analysis (Referee 1), (2) the applied benthic stable isotope correlation (Referee 2), and (3) the presentation of the data in Figure 4 (Referee 1 +2).

In the following, we would like to give a detailed explanation concerning the comments and recommendations given by the Reviewers, as well as the intended revisions in our revised manuscript.

Stefanie Kaboth, on behalf of all co-authors

## **Referee 1**

### *1.) Chapter Spectral Analysis & Precession control on MOW strength during the Early Pleistocene*

As requested by Referee 1, we have improved our spectral analysis by including wavelet analysis for both investigated intervals. These new results supplement the findings of the power spectra by clearly showing the dominance and stability of the (semi-)precession signal in the grain-size variability at Site U1389 during the Early Pleistocene. We have emphasized this finding accordingly in section 4.2 (Line 300 to 303) of our revised manuscript. The wavelets for both investigated intervals have been added to Figure 5 as Figures 5C and 5D. These adaptations are also in line with suggestions made by Referee 2 (see below), and we have now also included the findings of Becker et al. (2006, 2005) about precession related signals in the Eastern Mediterranean Sea during interval I (see Line 305 to 308). The methodological description of the wavelet analysis has been added to the Method section 2.7 (Line 185 to 187).

### *2.) Chapter Glacial-Interglacial change*

We believe that the MIS102 interval is robust in its present version and no further adaptations are necessary. Following the age constrain of MIS 102 according to Lisiecki and Raymo, (2005) the interval extends from 2.575 to 2.554 Ma. Through the initial age model based on bio- and magnetostratigraphy (see Table 1) the age interval between 2.5 and 2.581 Ma is very well constrained.

In contrast to Referee 1, we argue that the grain-size variability is a reliable representation for MOW variability during our investigated intervals despite in-part low recovery and sample resolution. As stated in the manuscript (see Lines 157 to 163) the grain-size proxy has been successfully used for Late Pleistocene studies (i.e. Kaboth et al. 2017, 2016). We think that the argued absolute amplitude reduction in MOW flow strength between interval I and II (see Lines 280 to 282) is also visible in Figure 4D and does not rely solely on the calculated relative change in amplitude expressed in Line 280.

We also believe that the description of the change in  $\delta^{13}\text{C}$  through North Atlantic water influence is sufficient in its current state (see Line 274 to 280).

### *3.) Chapter: Did Mow contribute to the Early Pleistocene climate transition?*

The occurrence of *Neogloboquadrina atlantica* (sin) is now clearly denoted in the revised Figure 4A by arrows at mid-point level of-MIS 100, 98, 96 at Site U1389. The reference for abundance patterns of *N. atlantica* in the eastern Mediterranean Sea and North Atlantic are

already provided in the discussion section 4.3 (Lines 379). The south Atlantic SST record of Site ODP 1090 has been added to Figure 4A following Bell et al. (2015) (this also aligns with suggestions made by Referee 2, see below).

### *Figures*

- 1.) Figure 1C highlighting the Mediterranean Sea circulation has been added. Caption changes have been made accordingly.
- 2.) Figure 3: Indeed, the correlation arrow for MIS 101 in Figure 3A has been revised. The dotted line indicating the mean sedimentation rate in Figure 3C has been removed.
- 3.) In the now revised Figure 4 we have unified the age notations between Figure 4 and Table 1. The mid-point levels of sapropels throughout the investigated intervals are already clearly highlighted in Figure 4D and we do not think it necessary to add them again to Figure 4B. We have added data pointer to the grain-size record in Figure 4D to better visualize the existing gaps in the record.
- 4.) Figure 5: Red noise level has been added to Figure 5A and 5B. Caption changes have been made accordingly.

### *Table*

- 1.) In the now revised version of the Table 1 we have listed the full species names of the biostratigraphic markers. The citation Raffi et al. (2006) has been added in the reference list.

## **Referee 2**

### *Major comments*

- 1.) As stated under Lines 232 to 234 in our initial manuscript, the argument regarding the intensification AMOC is based on the findings by Bell et al. (2015) and not just the SST data published by Lawrence et al. (2009) and shown in our Figure 4A. Including the SST record in Figure 4 is for orientation purposes of the reader as to the onset of the probed “plateau” in the North Atlantic SST development. The arguments made in Bell et al. (2015) are based already on a wide spread analysis of SST records across the North Atlantic including Sites (ODP Sites 607, 1090, 1082 and 982). However, we agree with Referee 2 and included the studies by Khélifi and Frank (2014) and Lisiecki (2014) (Line 365 to 372). These authors highlighted the lack of increased overturning circulation in the deep water opposed to the increased overturning postulated by Bell et al. (2015) in relation to the surface water trajectory. In our opinion this strongly argues for the effect of MOW on the intermediate branch of overturning circulation, a scenario already highlighted in Bahr et al. (2015) for MIS 5. This argument will have been newly added into the revised manuscript (under subsection 4.3, Line 365 to 372) and complement the existing argument of the prevalence of MOW along intermediate water depth within the North Atlantic by Loubere (1987) which was already included in the initial manuscript.
- 2.) The  $\delta^{18}\text{O}$  correction between both benthic species for the Early Pleistocene is  $y=1.06x-0.17$  ( $R^2=0.80$ ). Hence, the slope of the linear relationship is  $\sim 1$  and the y-intercept is minor considering the analytical error of the measurements which is  $\pm 0.08\text{‰}$ . This suggests a comparable oxygen isotope fractionation between *Planulina ariminensis* and *Cibicidoides ungerianus*. A similar behaviour has been postulated for *P. ariminensis* and other *Cibicidoides* species (e.g. Marchitto et al. 2014). For  $\delta^{13}\text{C}$ , the computed correction factor for both benthic species during the Early Pleistocene is  $y=0.13x+0.84$  ( $R^2=0.02$ ). Following the suggestion of Referee 2, we have reanalysed our data for a possible climate driven bias. Firstly, the samples utilized for the analysis of the interspecies correction were not specifically chosen for their warm/cold climatic background but under the premise that both benthic species were present in sufficient numbers for stable isotope analysis. Hence, the suggested form of analysis leads to the exclusion of  $\sim 25\%$  ( $n=20$ ) samples from the original data set corresponding to transitional climate conditions. This exclusion changes the inter species correlation to

$y=-0.02x+0.83$  ( $R^2< 0.02$ ). The correlation for only “warm” climatic conditions (corresponding light  $\delta^{18}\text{O}$  values) shifts the interspecies correlation to  $y=0.005x+0.83$  ( $R^2<0.02$ ;  $n=26$ ). Similar, the correlation for only “cold” climatic conditions (corresponding heavy  $\delta^{18}\text{O}$  values) shifts the interspecies correlation to  $y=-0.04x+0.84$  ( $R^2<0.02$ ;  $n=29$ ). Hence, it becomes obvious that no climatic driven bias can be found. We argue instead that the high scatter might relate to the variability of *C. ungerianus* from a preferably epifaunal to a very shallow infaunal life style in correspondence to different nutrient fluxes, oxygenation state, habitat changes etc. This would cause an enhanced variability in the  $\delta^{13}\text{C}$  microhabitat-offset between both species. Such variability has been observed at recent for other *Cibicidoides* species (Fontanier et al., 2006). In contrast, *P. ariminensis* has been argued to be a reliable recorder of the  $\delta^{13}\text{C}$  signal of MOW (Zahn et al., 1987; already stated on Lines 83 to 85 in the initial manuscript) and aligns with findings of e.g., Schönfeld (2002), Rogerson et al. (2011) and García-Gallardo et al. (2017) further suggesting that *P. ariminensis* is a true “elevated” epifaunal living species directly recording MOW properties. Specifically, the influence of remineralisation of sedimentary carbon on benthic  $\delta^{13}\text{C}$  which may overprint the MOW signal was discussed by Rogerson et al. (2011). The authors considered the  $\delta^{13}\text{C}$  signal ambiguous for most benthic foraminifera with the exception of *P. ariminensis* which showed the highest (positive) correlation with MOW flow strength.

We have added the additional information regarding the  $\delta^{18}\text{O}$  and  $\delta^{13}\text{C}$  signals at Site U1389 to section 2.3 of our revised manuscript with the exception of the climatic bias as simply no evidence for this could be found (as outlined above). The reference in the caption of Figure 4 to Kaboth et al., *in prep.* was a typo and has been removed. Only the stated inter species relations were applied in this study.

- 3.) We agree with the Referee 2 and have now included the findings of Becker et al. (2006, 2005) on precession influence on climate variability during MIS 100 in the Mediterranean Sea into the revised manuscript under subsection 4.2 (Line 305 to 308).
- 4.) Vertical movements of the MOW plume are an important mechanism as stated by Referee 2. However, the Late Pleistocene study of Bahr et al. (2015) has shown that Site U1389 is generally less prone to vertical movement than sites further up the shelf even under much more severe sea level variability than during the Early Pleistocene. The validity of utilizing  $\delta^{18}\text{O}$  to trace MOW prevalence in the Gulf of Cadiz has been already established in Kaboth et al. (2016). This approach argues that MOW is the

dominant water mass at the site with the heaviest oxygen isotopic signal compared to ambient North Atlantic water due to its density. We have highlighted this statement by revising Figure 1 of our manuscript and added the modern vertical water mass distribution along T, S and  $\delta^{18}\text{O}_w$  profiles for Site U1389 as Figure 1D. Based on this assumption the isotopic differences between the  $\delta^{18}\text{O}$  of the Mediterranean Sea (input signal) and the Gulf of Cadiz (output signal) reflects MOW variability as the ice volume contribution for the same time interval in both stable oxygen isotope records can be assumed to be identical. As the isotopic gradient in  $\delta^{18}\text{O}$  are generally small throughout both intervals it seems feasible to argue that MOW prevailed throughout our studied time frame. We have now outlined this approach in more detail in the revised manuscript in Line 245 to 257. The grain-size and  $\delta^{13}\text{C}$  gradient for both intervals give indication that the intensification of MOW occurred as outlined in subsection 4.1 of the manuscript. No further additions have been made.

#### *Minor comments*

- 1.) We have followed the suggestion by Referee 2 and changed the title into: “Mediterranean Outflow variability during the Early Pleistocene”
- 2.) Following the suggestions by Referee 2 we have added more details on sequence stratigraphy and paleo-water depth of the Singa/Vrica sections in a newly designed subsection 2.2 under Material & Methods (Line 105 to 114). It seemed more befitting to add additional information for the reader about the Singa/Vrica section in the Material section rather than into the Introduction as suggested by the Referee.
- 3.) Line 112-118 (initial manuscript): The high variability at Site U1389 in sedimentation rate is not unusual if compared to findings from the same site during the Late Pleistocene which shows a similar range (see Figure DR2 in Bahr et al. 2015). Generally, contourites are very dynamic depositional systems which is reflected in the evolution of sedimentation rates through time (Hernandez-Molina et al., 2014). No further changes have been made to the revised manuscript.
- 4.) Line 216 (initial manuscript): Yes, the black starts in the initial version of Figure 4B indicated the occurrences of *N. atlantica* during cold periods in Interval I. In accordance to the suggestions made also by Referee 1 (see above) we have modified Figure 4B to improve the visual occurrence pattern of *N. atlantica* to the reader.

- 5.) Line 263 (initial manuscript): We do not make this argument based on our data but instead this is based on the findings of Bell et al. (2015) as clearly stated in Line 363 to 365.
- 6.) The superscription of  $\delta^{18}\text{O}$  and  $\delta^{13}\text{C}$  has been checked in the revised manuscript.
- 7.) We have added to Figure 1: the location map of Singa/Vrica sections under 1B, a schematic of the Mediterranean circulation under 1C, and the modern vertical water mass profile at Site U1389 including T, S, and  $\delta^{18}\text{O}$  under 1D.
- 8.) We have highlighted in Figure 2A and B which represents stable oxygen and carbon isotope correlations.
- 9.) Figure 3: Commas have been replaced by dots.
- 10.) We believe Figure 4 has been visually improved to better reflect the content of the manuscript and aid the reader. As also suggested by Referee 1 we have added the South Atlantic SST record ODP 1090 to highlight the discussed intensification of AMOC (Bell et al. 2015). Furthermore, we have clarified the occurrence of *N. atlantica* (also see Referee 2 comments on Line 216 and Referee 1), and also visually improved the time range of the studied intervals in relation to the shown SST records.

## References

- Bahr, A., Kaboth, S., Jiménez-Espejo, F.J., Sierro, F.J., Voelker, A.H.L., Lourens, L., Röhl, U., Reichart, G.J., Escutia, C., Hernández-Molina, F.J., Pross, J., and Friedrich, O., 2015, Persistent monsoonal forcing of Mediterranean Outflow Water dynamics during the late Pleistocene: *Geology*, v. 43, p. 951–954, doi: 10.1130/G37013.1.
- Becker, J., Lourens, L.J., Hilgen, F.J., van derLaan, E., Kouwenhoven, T.J., and Reichart, G.-J., 2005, Late Pliocene climate variability on Milankovitch to millennial time scales: A high-resolution study of MIS100 from the Mediterranean: *Palaeogeography, Palaeoclimatology, Palaeoecology*, v. 228, p. 338–360, doi: 10.1016/j.palaeo.2005.06.020.
- Becker, J., Lourens, L.J., and Raymo, M.E., 2006, High-frequency climate linkages between the North Atlantic and the Mediterranean during marine oxygen isotope stage 100 (MIS100): ATLANTIC MEDITERRANEAN LINKAGE: *Paleoceanography*, v. 21, p. PA3002, doi: 10.1029/2005PA001168.
- Bell, D.B., Jung, S.J.A., and Kroon, D., 2015, The Plio-Pleistocene development of Atlantic deep-water circulation and its influence on climate trends: *Quaternary Science Reviews*, v. 123, p. 265–282, doi: 10.1016/j.quascirev.2015.06.026.
- Fontanier, C., Mackensen, A., Jorissen, F.J., Anschutz, P., Licari, L., and Griveaud, C., 2006, Stable oxygen and carbon isotopes of live benthic foraminifera from the Bay of Biscay: Microhabitat impact and seasonal variability: *Marine Micropaleontology*, v. 58, p. 159–183, doi: 10.1016/j.marmicro.2005.09.004.

- García-Gallardo, Á., Grunert, P., Van derSchee, M., Sierro, F.J., Jiménez-Espejo, F.J., Alvarez Zarikian, C.A., and Pillar, W.E., 2017, Benthic foraminifera-based reconstruction of the first Mediterranean-Atlantic exchange in the early Pliocene Gulf of Cadiz: *Palaeogeography, Palaeoclimatology, Palaeoecology*, v. 472, p. 93–107, doi: 10.1016/j.palaeo.2017.02.009.
- Hernandez-Molina, F.J., Stow, D.A.V., Alvarez-Zarikian, C.A., Acton, G., Bahr, A., Balestra, B., Ducassou, E., Flood, R., Flores, J.-A., Furota, S., Grunert, P., Hodell, D., Jimenez-Espejo, F., Kim, J.K., et al., 2014, Onset of Mediterranean outflow into the North Atlantic: *Science*, v. 344, p. 1244–1250, doi: 10.1126/science.1251306.
- Kaboth, S., Lourens, L., and Departement Aardwetenschappen (Utrecht), 2016, Deciphering the paleoceanographic and paleoclimatic evolution of the Gulf of Cádiz during the past 2.6 million years.
- Khélifi, N., and Frank, M., 2014, A major change in North Atlantic deep water circulation 1.6 million years ago: *Climate of the Past*, v. 10, p. 1441–1451, doi: 10.5194/cp-10-1441-2014.
- Lawrence, K.T., Herbert, T.D., Brown, C.M., Raymo, M.E., and Haywood, A.M., 2009, High-amplitude variations in North Atlantic sea surface temperature during the early Pliocene warm period: VARIABLE PLIOCENE NORTH ATLANTIC SSTs: *Paleoceanography*, v. 24, p. n/a-n/a, doi: 10.1029/2008PA001669.
- Lisiecki, L.E., 2014, Atlantic overturning responses to obliquity and precession over the last 3 Myr: *Paleoceanography*, v. 29, p. 71–86, doi: 10.1002/2013PA002505.
- Lisiecki, L.E., and Raymo, M.E., 2005, A Pliocene-Pleistocene stack of 57 globally distributed benthic  $\delta^{18}\text{O}$  records: *Paleoceanography*, v. 20, p. 1–17, doi: 10.1029/2004PA001071.
- Loubere, P., 1987, Changes in mid-depth North Atlantic and Mediterranean circulation during the Late Pliocene — Isotopic and sedimentological evidence: *Marine Geology*, v. 77, p. 15–38, doi: 10.1016/0025-3227(87)90081-8.
- Marchitto, T.M., Curry, W.B., Lynch-Stieglitz, J., Bryan, S.P., Cobb, K.M., and Lund, D.C., 2014, Improved oxygen isotope temperature calibrations for cosmopolitan benthic foraminifera: *Geochimica et Cosmochimica Acta*, v. 130, p. 1–11, doi: 10.1016/j.gca.2013.12.034.
- Raffi, I., Backman, J., Fornaciari, E., Pälike, H., Rio, D., Lourens, L., and Hilgen, F., 2006, A review of calcareous nannofossil astrobiochronology encompassing the past 25 million years☆: *Quaternary Science Reviews*, v. 25, p. 3113–3137, doi: 10.1016/j.quascirev.2006.07.007.
- Rogerson, M., Schönfeld, J., and Leng, M.J., 2011, Qualitative and quantitative approaches in palaeohydrography: A case study from core-top parameters in the Gulf of Cadiz: *Marine Geology*, v. 280, p. 150–167, doi: 10.1016/j.margeo.2010.12.008.
- Schönfeld, J., 2002, A new benthic foraminiferal proxy for near-bottom current velocities in the Gulf of Cadiz, northeastern Atlantic Ocean: Deep-Sea Research Part I: *Oceanographic Research Papers*, v. 49, p. 1853–1875, doi: 10.1016/S0967-0637(02)00088-2.
- Zahn, R., Sarnthein, M., and Erlenkeuser, H., 1987, Benthic isotope evidence for changes of the Mediterranean outflow during the Late Quaternary: *Paleoceanography*, v. 2, p. 543–559, doi: 10.1029/PA002i006p00543.



# Mediterranean Outflow Water variability during the Early Pleistocene

Stefanie Kaboth<sup>1,2</sup>, Patrick Grunert<sup>3</sup>, Lucas J. Lourens<sup>2</sup>

<sup>1</sup> Department of Earth Sciences, National Taiwan University, No 1. Sec. 4 Roosevelt Road,  
106 Taipei City, Taiwan

<sup>2</sup> Department of Earth Sciences, Utrecht University, Heidelberglaan 2, 3584 CS, Utrecht, The  
Netherlands

<sup>3</sup> Institute of Earth Sciences, University of Graz, NAWI Graz, Heinrichstraße 26, 8010 Graz,  
Austria

Correspondence to: Stefanie Kaboth ([stefaniekaboth@ntu.edu.tw](mailto:stefaniekaboth@ntu.edu.tw))

## Abstract

Gaining insights into the evolution of Mediterranean Outflow Water (MOW) during the Early Pleistocene has been so far hampered by the lack of available paleoclimatic archives. Here we present the first benthic foraminifera stable oxygen and carbon isotope records and grain-size data from IODP Expedition 339 Site U1389 presently located within the upper core of the MOW in the Gulf of Cadiz for the time interval between 2.6 and 1.8 Ma. A comparison with an intermediate water mass record from the Mediterranean Sea strongly suggest an active MOW supplying Site U1389 on glacial-interglacial timescales during the Early Pleistocene. We also find indication that the increasing presence of MOW in the Gulf of Cadiz during the investigated time interval aligns with the progressive northward protrusion of Mediterranean sourced intermediate water masses into the North Atlantic, possibly modulating the intensification of the North Atlantic Meridional Overturning Circulation at the same time. Additionally, our results suggest that MOW flow strength was already governed by precession and semi-precession cyclicity during the Early Pleistocene against the background of glacial-interglacial variability.

Keywords: Mediterranean Outflow, Early Pleistocene, Atlantic Meridional Overturning Circulation, Sapropel

## 1. Introduction

The Mediterranean Outflow Water (MOW) is a distinct hydrographic feature at intermediate water depths in the Gulf of Cadiz, distinguished from other ambient North Atlantic water masses by its warm and saline character (Fig. 1A, Ambar and Howe, 1979; Bryden et al., 1994; Bryden and Stommel, 1984). In the modern hydro-climatic setting of the Mediterranean Sea the MOW is predominately sourced by Levantine Intermediate Water (~70%), formed in the Eastern Mediterranean Basin, and variable parts of Western Mediterranean Deep Water (WMDW) originating in the Alboran and Tyrrhenian Sea (Fig. 1B and C, Millot, 2014, 2009; Millot et al., 2006). After exiting the Strait of Gibraltar, the MOW plume cascades down the continental slope due to its increased density (Ambar and Howe, 1979; Hernandez-Molina et al., 2014a; Hernández-Molina et al., 2006; Mulder et al., 2006). In the Gulf of Cadiz, MOW follows the topography of the continental shelf in two major flow cores at 800-1400 m water depth (lower MOW core), and 500-700 m water depth including our study area (upper MOW core, Fig. 1A) (Baringer and Price, 1997; Borenäs et al., 2002; Hernández-Molina et al., 2013). After exiting the Gulf of Cadiz, most of MOW flows north along the European continental margin until it mixes with the North Atlantic Current at Rockall Plateau (Hernandez-Molina et al., 2014b). Beyond the Mediterranean region, MOW has been acknowledged as an important modulator of the North Atlantic salt budget with previous research suggesting that the absence of MOW may reduce Atlantic Meridional Overturning Circulation (AMOC) by as much as 15% compared to modern (Rogerson et al., 2006). Despite its potential cosmopolitan significance, the paleoceanographic history of MOW has so far been only studied for the Pliocene (Khelifi et al., 2009; Khélifi and Frank, 2014), and during the late and mid-Pleistocene (Bahr et al., 2015; Kaboth et al., 2016, 2017; Llave et al., 2006; Schönfeld, 2002; Schönfeld and Zahn, 2000; Toucanne et al., 2007; Voelker et al., 2006). In this light, the reconstruction of MOW variability might be particularly interesting in the broader view of the Pliocene-Pleistocene climate transition. The early Pleistocene period spans the transition from the preceding Pliocene climate optimum with limited ice sheets in the Northern Hemisphere to the cooler Middle and Late Pleistocene climate with rapidly developing continental ice growth in both hemispheres (Raymo et al., 1992; Shackleton and Hall, 1984). Throughout the Early

Pleistocene, however, an interruption of the long-term Northern Hemisphere ice volume increase can be observed in concert with a sea-surface temperature stabilization in the high latitude North Atlantic cooling trend (Bell et al., 2015). It was suggested that these changes relate to an increase in AMOC strength, and in extension, an increase in northward heat transport (Bell et al., 2015). Here we elaborate on the possible role of MOW on North Atlantic Paleoceanographic changes during the early Pleistocene climate transition by investigating the benthic foraminifera stable oxygen and carbon isotopes and grain-sizes from IODP 339 Site U1389, located on the upper slope of the Gulf of Cadiz (see Fig. 1A) for two time intervals: 2.6 and 2.4 Ma and 2.1 and 1.8 Ma. We have compared our new data with the benthic stable isotope record of the Singa/Vrica sections in Calabria (Italy), representing the intermediate water mass end-member of the Mediterranean Sea (Lourens et al., 1996a, 1996b; unpublished data) that serves as a reference for the source region of MOW during the Early Pleistocene (Fig. 1B). Our results bridge the gap in our understanding of MOW variability between the wider researched Pliocene and Late and Middle Pleistocene. We aim to shed new light on MOW variability during the Early Pleistocene by analysing hydrographic changes within the Mediterranean source region, investigating the low-latitude control of MOW against the background of dominant obliquity controlled glacial-interglacial cyclicity, and documenting the potential influence of MOW variability on long-term climatic oscillations in the North Atlantic.

## 2. Material & Methods

### 2.1 Site U1389

Integrated Ocean Drilling Program (IODP) Site U1389 (36°25.515'N; 7°16.683'W) was drilled in December 2011 and January 2012 during Expedition 339 (Stow et al., 2013). It is located on the southern Iberian Margin ~90 km west of the city of Cadiz and perched on the northwest side of the Guadalquivir diapiric ridge in 644 m water depth (Fig. 1A). At present, IODP Site U1389 is at depth directly influenced by the upper MOW core (Hernández-Molina et al., 2013). In its modern configuration MOW (>36 PSU, ~13°C) is sourced predominately of intermediate water masses from the Eastern Mediterranean Sea (Fig. 1D, Ambar and Howe, 1979; Millot, 2009, 2014; Millot et al., 2006). The water column above the MOW is influenced by subtropical water masses (14-16°C; ~36.2 PSU) originating from the northern boundary of the eastern Azores Current branch (Peliz et al., 2009, 2005). During spring and summer, colder

and fresher subsurface water masses can be traced along the upper and middle slope as indicated by a salinity minimum above the MOW (see Fig. 1D) linked to the seasonal upwelling systems along the Iberian Margin (Fiúza et al., 1998).

For the present study we analysed 423 samples from Site U1389 Hole E which cover the Early Pleistocene (2.6 to 1.8 Ma) time interval at 30 cm intervals between 549.8 to 706.35 mbsf. An expanded hiatus at Hole U1389E between 2.1 and 2.4 Ma (~622-644 mbsf) has been initially related to a phase of highly active MOW (Hernández-Molina et al., 2013; Stow et al., 2013). However, more recent findings link this compressional event to tectonically invoked erosion (Hernández-Molina et al., 2015). As a consequence, we present the data split in two intervals (Interval I: 2.6-2.4 Myr and II: 2.1 to 1.8 Myr).

## 2.2 Singa and Vrica

The Monte Singa IV and Vrica sections of Early Pleistocene age contain sequences of marine marls and sapropelic clay layers, which are exposed in Calabria, southern Italy (Lourens et al., 1992). During the time of deposition, both sections have been part of the continental slope bordering the Ionian basin. The benthic foraminiferal associations represent a deep bathyal paleoenvironment between ~900 to ~1100 m water depth (Verhallen, 1991). This suggests that the benthic isotope data derived from these sediment sequences recorded intermediate water mass conditions within the eastern Mediterranean Sea. The biostratigraphic correlation indicates that the Vrica sapropelite suite is equivalent to the IV sequence at Monte Singa (Verhallen, 1991; Zijderveld et al., 1991).

## 2.3 Stable isotope measurements and interspecies correction

The freeze-dried sediment samples of Site U1389 were wet sieved into three fractions (>150  $\mu\text{m}$ , 150-63 $\mu\text{m}$ , 63-38  $\mu\text{m}$ ), and their residues oven dried at 40°C. Stable oxygen ( $\delta^{18}\text{O}$ ) and carbon ( $\delta^{13}\text{C}$ ) isotope analyses were carried out on 4 to 6 specimens of the epifaunal living foraminiferal species *Planulina ariminensis* and *Cibicidoides ungerianus* from the >150  $\mu\text{m}$  size fraction. All selected specimens were crushed, sonicated in ethanol, and dried at 35°C. Stable isotope analyses were carried out on a CARBO-KIEL automated carbonate preparation device linked to a Thermo-Finnigan MAT253 mass spectrometer at Utrecht University. The precision of the measurements is  $\pm 0.08\text{‰}$  for  $\delta^{18}\text{O}$  and  $\pm 0.03$  for  $\delta^{13}\text{C}$ . The results were calibrated using the international standard NBS-19, and the in-house standard NAXOS.

Isotopic values are reported in standard delta notation ( $\delta$ ) relative to the Vienna Pee Dee Belemnite (VPDB). *P. ariminensis* was absent in 100 samples; resulting gaps were filled with *C. ungerianus* values corrected for interspecies isotopic offsets. The calculation of the interspecies offset is based on 62 paired isotope measurements of both benthic species. The  $\delta^{18}\text{O}$  interspecies offset was determined by applying a least square linear regression equation (Fig. 2). The Pearson correlation coefficient ( $R^2$ ) between both species shows high correlation of 0.80 for  $\delta^{18}\text{O}$  (Fig. 2A). The calculated slope of this relationship is  $\sim 1$  with an y-intercept of +0.10 ‰ which is minor considering the analytical error of the measurements of  $\pm 0.08\%$ . This suggests a comparable oxygen isotope fractionation between *P. ariminensis* and *C. ungerianus*. A similar behaviour has been postulated for *P. ariminensis* and other *Cibicidoides* species (Marchitto et al., 2014). These results also align with findings from the same benthic species during the Late and Middle Pleistocene (Kaboth et al., 2017). In contrast, the  $\delta^{13}\text{C}$  correlation factor for both benthic species during the Early Pleistocene is insignificant  $R^2=0.02$  (Fig. 2B). We argue that the high scatter of *C. ungerianus* during the Early Pleistocene might relate to the variability from a preferably epifaunal to a very shallow infaunal life style in correspondence to different nutrient fluxes, oxygenation state, habitat changes etc. This would cause an enhanced variability in the  $\delta^{13}\text{C}$  microhabitat-offset between both species. Such variability has been observed at recent for other *Cibicidoides* species (Fontanier et al., 2006). In contrast, *P. ariminensis* has been argued to be a reliable recorder of the  $\delta^{13}\text{C}$  signal of MOW (Zahn et al., 1987). Rogerson et al. (2011), Schönfeld (2002) and García-Gallardo et al. (2017) further suggesting that *P. ariminensis* is a true “elevated” epifaunal living species directly recording MOW properties. Specifically, the influence of remineralisation of sedimentary carbon on benthic  $\delta^{13}\text{C}$  which may overprint the MOW signal was discussed by Rogerson et al. (2011). The authors considered the  $\delta^{13}\text{C}$  signal ambiguous for most benthic foraminifera with the exception of *P. ariminensis* which showed the highest (positive) correlation with MOW flow strength. Therefore, we only present the  $\delta^{13}\text{C}$  of *P. ariminensis*, considered a valuable basis for  $\delta^{13}\text{C}$  studies of the paleo-hydrography of the MOW.

## 2.4 Grain-size analyses

The stable isotope sample preparation was used to obtain weight percentages (wt.-%) of the grain-size fractions  $>150\ \mu\text{m}$ ,  $150\text{--}63\ \mu\text{m}$ ,  $63\text{--}38\ \mu\text{m}$  and  $<38\ \mu\text{m}$  for the investigated samples were obtained during sample preparation for isotope analyses. We concentrate on the grain-

size fraction between 63-150  $\mu\text{m}$  which has been used previously as indicator for flow strength changes in the Gulf of Cadiz attributed to MOW variability (Rogerson et al., 2005). Even though untreated weight percentages hold a bias it has been shown for the last climatic cycle that weight percentages mirror major peaks in Zr/Al records, considered a reliable recorder of MOW flow strength variability (Bahr et al., 2014), and thus can be used to trace MOW intensity patterns (Kaboth et al., 2016, 2017).

## 2.5 Chronology

Primary age constraints are based on paleomagnetic and biostratigraphic tie points as listed in Table 1. The secondary age model follows the visual correlation of the benthic  $\delta^{18}\text{O}$  record at Site U1389 to the benthic  $\delta^{18}\text{O}$  “MedSea” stack of Lourens et al. (unpublished data) within the investigated time period. The MedSea stack is based on the benthic *C. ungerianus*  $\delta^{18}\text{O}$  values from the Singa and Vrica sections located in Calabria, Italy derived from the same samples used for the planktic  $\delta^{18}\text{O}$  record in Lourens et al., (1996a, pers. comm.). The stable isotope measurements for the MedSea stack were carried analogous the protocol described in section 2.2 (Lourens, pers. comm.) The *C. ungerianus* values of the MedSea stack were adjusted to the *P. ariminensis* based  $\delta^{18}\text{O}$  record at Site U1389 by applying the interspecies correction equation cited under section 2.2 and Figure 2A. The Mediterranean Sea stack  $\delta^{18}\text{O}$  time series is based on tuning sapropel midpoints to La2004 65° N summer insolation maxima, including a 3-kyr time lag (Lourens, 2004). Monitoring of the sedimentation rate was done to control viability of secondary age model. The designation of MIS stages follows the MedSea stack chronology (Lourens, 2004). The respective tie points of the secondary age model are listed in Table 2.

## 2.7 Spectral Analysis

Spectral analysis was performed to test for statistically significant cycles with respect to orbital parameters. For analysis of orbital periodicities, the non-constantly sampled time series were analysed by a Multi Taper Method using the program REDFIT (Schulz and Mudelsee, 2002). Morlet wavelets assuming a 10% red noise level were calculated following the methods described in Grinsted et al. (2004), Liu et al. (2007) and Torrence and Compo (1998) by applying the ‘biwavelet’ R package (Gouhier et al., 2016; R Core Team, 2014).

## 3 Results

### 3.1 Age model & Sedimentation rates

The two studied intervals of the Site U1389  $\delta^{18}\text{O}$  record exhibit similar glacial-interglacial variability as present in MedSea stack throughout the Early Pleistocene. The estimated mean sedimentation rate for both intervals is  $\sim 0.30$  m/kyr which is similar to the sedimentation rate of  $\sim 0.25$  to  $\sim 0.30$  m/kyr that has been calculated from shipboard stratigraphy for the past 3.2 Myr (Hernández-Molina et al., 2013; Stow et al., 2013). A doubling or tripling of the sedimentation rate coincides with transition of MIS 103, MIS 101 to MIS 100 and interglacials MIS 99 and MIS 97 in Interval I, and  $\sim$ MIS 68 in Interval II. Condensed sections with low sedimentation rates of  $\sim 0.1$  m/kyr correlate with the transition between MIS 98 to MIS 97 and MIS 95 in Interval I, and MIS 78 to MIS 75 in Interval II, respectively. Generally, the high amplitude changes of the sedimentation rate at Site U1389 during the Early Pleistocene is mimicked by a similar behaviour recorded during the Late Pleistocene (Bahr et al., 2015).

### 3.2 Stable oxygen and carbon isotopes

The comparison between both intervals of the  $\delta^{18}\text{O}$  record at Site U1389 with the benthic  $\delta^{18}\text{O}$  MedSea stack is shown in Figure 4. In Interval I, lightest values of 1.17 and 1.22 ‰ coincide with interglacials MIS 103 and 101, and the strongest glacial enrichment in  $\delta^{18}\text{O}$  (2.69 ‰) coincides with MIS 100. Transitional depletion is on average 0.97 ‰ with highest values (1.29 ‰) in the interval between MIS 101 and 100 (see Fig. 4). In Interval II, the lightest values coincide with MIS 73 (1.36 ‰) whereas the strongest glacial  $\delta^{18}\text{O}$  enrichment can be observed during MIS 78, 72 and 68 with 2.47 ‰, 2.42 ‰ and 2.69 ‰, respectively (see Fig. 4). Transitional depletion is on average 0.82 ‰ with highest values (1.06 ‰ and 1.19 ‰) in the interval between MIS 73 and 72, and the transition from MIS 69 to MIS 68. Pronounced amplitude offsets between the  $\delta^{18}\text{O}$  signal of Site U1389 and MedSea are visible in both intervals but especially during MIS 103, 102, 77, 75 and 67 (Fig.4). These perturbations are of the order of up to  $\sim 0.5$  ‰ (e.g. MIS 75). The comparison between both intervals of the  $\delta^{13}\text{C}$  record at Site U1389 with the  $\delta^{13}\text{C}$  MedSea stack is shown in Figure 4. During Interval I, lightest values of 0.27 and 0.32 ‰ coincide with MIS 101 and 100, and the heaviest values ( $\sim 1.27$  ‰) coincide with the transition of MIS 102 to MIS 101, MIS 100, and the transition



between MIS 99 to MIS 98. In Interval II, the lightest values correspond to MIS 74 (-0.02 ‰) and the transition between MIS 68 and 67 (-0.06 ‰). The heaviest  $\delta^{13}\text{C}$  values coincide with MIS 71 (1.56 ‰).

### 3.3 Grain-size

The mean grain-size values (63-150  $\mu\text{m}$ ) for both investigated intervals are  $\sim 8.0$  %-wt. Highest values of both investigated intervals of up to  $\sim 60$  %-wt. are correlated with MIS 100 and 77 (Fig. 4). The grain-size variability is seemingly not related to glacial-interglacial variability as a clear response of the grain-size to the variability of  $\delta^{18}\text{O}$  records at Site U1389 cannot be observed.

### 3.4 Spectral analyses

The grain-size records of Interval I and II at Site U1389 exhibit significance (80% to 90%) variance in the precession ( $\sim 23$  kyr), semi-precession ( $\sim 11$  kyr) and potentially 1/3-precession ( $\sim 7$  kyr; significant Interval II only) frequency band (Fig. 5A and B). The obliquity signal is insignificant in both investigated intervals. The wavelet analysis for Interval I (Fig. 5C) reveals that the precession and semi-precession signal is most dominant between 2.55 and 2.50 Myrs. The lack of stability in the precession band from 2.5 to 2.4 Ma correlates with the reduced sample resolution due to poor core recovery (see Fig. 3). During Interval II the precession and semi-precession signal is most dominant during the interval between 2.0 Ma and 1.9 Ma. Starting from 2.0 Ma the 1/3-precession signal is becoming increasingly more prominent and stable (Fig. 5D).

## 4. Discussion

### 4.1 Glacial-Interglacial MOW variability at Site U1389 during the Early Pleistocene

In order to utilize the  $\delta^{18}\text{O}$  signal at Site U1389 to trace MOW variability we assume that the global ice volume contributions of the  $\delta^{18}\text{O}$  signal within the same time interval for Site U1389 and the Mediterranean Sea are equal. Consequently, differences in  $\delta^{18}\text{O}$  are caused by temperature and/or salinity differences of the water masses between both sites. The modern heavy oxygen isotope signal of MOW (see Fig. 1D) is a consequence of its increased



temperature and salinity linked to its Mediterranean source region, and hence setting it apart from the isotopic lighter overflowing water masses of North Atlantic origin. Therefore, we argue that the similarities of the  $\delta^{18}\text{O}$  values between Site U1389 and the MedSea stack during Interval I (2.6-2.4 Ma) and Interval II (2.1-1.8 Ma) emphasizes the direct influence of MOW at Site U1389. In this sense, our findings also strongly suggest that MOW formation during the Early Pleistocene was similar to modern conditions where MOW originates largely from intermediate water masses such as the Levantine Intermediate Water (Millot, 2009, 2014; Millot et al., 2006). The  $\delta^{18}\text{O}$  difference between Site U1389 and the Mediterranean Sea is small during glacial periods in both investigated intervals, suggesting that Site U1389 bathed in MOW during these colder climatic conditions throughout the Early Pleistocene time interval (Fig. 4A). This is particularly interesting in light of the proposed vertical shift of the MOW flow path during glacial periods of the Late Pleistocene fostered by the increased density of the outflowing Mediterranean water masses (Kaboth et al., 2016; Lofi et al., 2015; Rogerson et al., 2005; Schönfeld and Zahn, 2000; Toucanne et al., 2007; Voelker et al., 2006). This suggests that Site U1389 was not subjected to major glacial-interglacial induced flow path changes during the early Pleistocene, possibly due to its deeper and relatively proximal location to the Strait of Gibraltar, placing it more into the general flow path of upper MOW. These results confirm the inferences derived from Site U1389 of the Late Pleistocene interval where MOW activity was also shown to be largely unaffected by glacial-interglacial variability but instead predominately influenced by insolation driven hydro-climatic changes of its Mediterranean source region (Bahr et al., 2015).

In contrast, the interglacial periods of both intervals show a small but relative depletion in the Mediterranean Sea compared to the  $\delta^{18}\text{O}$  signal at Site U1389 which might reflect relatively higher temperatures or lower salinity of the intermediate Mediterranean Sea waters with respect to the MOWs during interglacial periods. The strongest intervals of relative  $\delta^{18}\text{O}$  depletion throughout both investigated time periods correlate with MIS 103, 102, MIS 75 and MIS 67 characterized by a depletion of up to  $\sim 0.5$  ‰ in the Mediterranean Sea compared to Site U1389. This shift might correspond to a freshening of the Mediterranean Sea intermediate water column during sapropel formation and a consequently reduction of MOW influence at Site U1389 (Rogerson et al., 2012). In case of MIS 102 and 67 sapropels have been documented in the Eastern Mediterranean Sea basin but not for MIS 75 (Emeis et al., 2000; Lourens, 2004; Lourens et al., 1992, 1996a). During Interval II, the generally heavier  $\delta^{13}\text{C}$  values at U1389 are close to those of the Mediterranean Sea values inferring that MOW was in fact the predominant source of bottom water at Site U1389 between 1.8 and 2.1 Ma (Fig. 4C). In contrast, the older

Interval I is characterized by a slightly increased  $\delta^{13}\text{C}$  gradient between Site U1389 and the Mediterranean Sea suggesting a generally larger contribution of ambient North Atlantic water masses carrying a lighter  $\delta^{13}\text{C}$  signal to the site. This could indicate a more vigorous MOW or that during Interval I the MOW flow core was less proximal than during Interval II. The later argument seems to be supported by the grain-size and its variability, as Interval II shows a  $\sim 10\%$  decrease in mean and amplitude relative to Interval I (Fig. 4D). This would suggest that during Interval I Site U1389 was less proximal to the flow core albeit more sensitive to flow strength changes whereas during Interval II the MOW plume has settled upon Site U1389. This is further supported by findings from seismic records in the Gulf of Cadiz that also suggest that at  $\sim 2.1$  Ma the present day circulation established (Hernandez-Molina et al., 2014b).

A distinct increase in the  $\delta^{13}\text{C}$  gradient can be seen during MIS 96, which may document a particular strong MOW activity. However, the sample resolution during MIS 96 and the subsequent MIS 95 is relatively low so that increase in the  $\delta^{13}\text{C}$  gradient remains ambiguous. The onset of the subsequent hiatus which has been argued to represent depositional erosion due to increased bottom current activity of the MOW could argue for a strong intensification of MOW activity (Hernandez-Molina et al., 2014b).

#### 4.2 Precession control on MOW strength during the Early Pleistocene: Similarities to Late Pleistocene MOW behaviour?

Untreated grain-size weight percentages can only give an indication for patterns in flow strength (Kaboth et al., 2016, 2017). For the two investigated intervals we find that the 63-150  $\mu\text{m}$  fraction variability is seemingly modulated by a  $\sim 23$  kyr pacing (Fig. 4D). This relationship is evident in the power spectrum of the grain-size data which yields for both intervals a dominance in the precession and semi-precession frequency band ( $\sim 23$  and  $\sim 11$  kyr) (Fig. 5A and B). The dominance and stability of the recorded precessional and semi-precessional signal in the grain-size variability throughout both investigated intervals is also highlighted by the wavelet analysis (Fig. 5C and D). This suggests that the flow strength of MOW was probably directly modulated by precession during the Early Pleistocene, aligning with previous findings based on Zr/Al ratios at Site U1389 from the Late Pleistocene (Bahr et al., 2015). In fact, a strong precessional influence was also shown for  $\delta^{18}\text{O}$  records from the eastern Mediterranean Sea (ODP site 967 and 969) and the mid-latitude North Atlantic during MIS 100 to MIS 96 (Becker et al., 2005, 2006). For the late Pleistocene, an inverse relationship was found between precession and MOW dynamics (Bahr et al., 2015; Kaboth et al., 2016). During periods of

increased summer insolation at the time of precession minima, the monsoonal rain belts expand northward causing an increase of freshwater discharge by the river Nile (e.g. Rohling et al., 2015; Rossignol-Strick, 1983, 1985). This effectively impedes intermediate water mass formation in the Eastern Mediterranean, thereby suppressing MOW production. From the correlation of the filtered ~23 kyr signal to the grain-size variability at site U1389 a similar relationship already existed during both investigated intervals of the Early Pleistocene (Fig. 4D). We also find significant semi -precession (~11 kyr) influence indicative for a primarily low-latitude response argued to originate in the tropics (Rutherford and D'Hondt, 2000; de Winter et al., 2014).

The  $\delta^{18}\text{O}$  signal comparison of Site U1389 and the MedSea stack is also particularly interesting in the context of sapropel formation, as the MedSea stack due to its intermediate paleo-water depth was sensitive to freshwater induced changes in the intermediate water composition. A substantial freshening of the intermediate water masses in the Mediterranean Sea can be inferred from the strongly depleted  $\delta^{18}\text{O}$  values during MIS 103, 102, 77, 75 and 67 relative to Site U1389 (Fig. 4A). The potentially reduced MOW supply at Site U1389 at the same time would increase the isotopic gradient between both locations, as Site U1389 could be affected by more open ocean conditions. However, despite the low sample resolution, this seems not a persistent relationship throughout both investigated intervals. For the Holocene S1, the proposed reduction in MOW has been documented by the absence of sandy contourite layers from the middle slope of the Gulf of Cadiz indicating a sudden reduction in flow strength and sediment delivery by the MOW (Toucanne et al., 2007; Voelker et al., 2006). The grain-size values throughout both investigated intervals at Site U1389 are typically low during sapropel formation supporting the findings from the middle and upper slope during the Late Pleistocene (Kaboth et al., 2016). However, the grain -size is seemingly increased during the sapropels deposited in the Eastern Mediterranean Sea at ~1.92 and 1.85 Myrs (Fig. 4D). This in-phase behaviour could potentially be a tuning artefact or relate to the fact that numerical model simulations imply that remnant thermal driven overturning circulation still occurs throughout the most extreme freshening events in the eastern Mediterranean Sea (Myers, 2002). This would imply that during the sapropel formation at ~1.92 and 1.85 Myrs MOW was potentially still active at Site U1389.

#### 4.3 Did MOW contribute to the Early Pleistocene climate transition?

Between ~2.8 and 2.4 Myrs (Interval I) occurrences of *Neogloboquadrina atlantica* (sin), an extinct polar species, were reported in the Mediterranean Sea during glacial periods suggesting the intrusion of colder water masses into the Mediterranean basin (Becker et al., 2005; Lourens and Hilgen, 1997; Zachariasse et al., 1990). We also find *N. atlantica* (sin) present during glacial periods of Interval I (Fig. 4B), confirming a more southern delineation of transitional and subpolar water masses during glacial periods of the Early Pleistocene than in recent setting (Voelker et al., 2015). This latitudinal shift might have occurred in concert with a more sluggish AMOC at least during the glacial periods if not throughout the whole time interval (Bell et al., 2015). Colder and more arid background conditions in the Mediterranean Sea could foster a stronger MOW analogous to cold spells related to Heinrich Events throughout the last climatic cycle (Bahr et al., 2014, 2015; Kaboth et al., 2016). An intensification of MOW during Interval I would align with the increased  $\delta^{13}\text{C}$  gradient between Site U1389 and the Mediterranean Sea suggesting a more vigorous MOW which is also reflected by higher grain-size amplitudes compared to Interval II (Fig. 4C and D). Our data, however, do not extend further back in time to test whether these conditions coincides with the proposed steady increase of MOW activity in the Gulf of Cadiz since 3.2 Ma as inferred from natural gamma ray logs and seismic profiles (Hernández-Molina et al., 2015), and with the arrival of Mediterranean sourced intermediate water mass at North Atlantic Sites DSDP 548 and 552 and ODP 982 from ~3.6 onwards (Khélifi et al., 2014; Loubere, 1987). This northward protrusion of warm and saline MOW towards high-latitude deep-water convection hot spots is considered an important modulator of the North Atlantic salt budget (Bahr et al., 2015; Rogerson et al., 2006; Voelker et al., 2006). We suggest that steady contributions of MOW throughout Interval I supplied continuously salt into the North Atlantic and potentially preconditioned the strong AMOC activity phase starting at ~2.4 Ma (Bell et al., 2015) when a tipping point was reached (Fig. 4A). In this regard, Khélifi and Frank (2014) and Lisiecki (2014) suggested the lack of increased overturning circulation in the deep water during this time interval. This at first glance stands in contrast to the proposed increased overturning circulation postulated by Bell et al. (2015) in relation to changes in the North Atlantic surface water mass trajectory. We argue that the changes in the surface water masses potentially relate to an intensification in the intermediate not the deep-water branch of the overturning cell stimulated by the increased northward protrusion of MOW. Such a scenario was already highlighted in Bahr et al. (2015) for MIS 5 and Late Pleistocene climatic conditions. Hence, the Early Pleistocene MOW might have acted as a positive climatic feedback mechanism against the background of increasingly colder temperatures. This contrasts the

warm Pliocene setting where it was proposed that MOW contributions to the North Atlantic did not have a significant influence on the AMOC (Khélifi et al., 2014).

The intensification of the AMOC is also in concert with the disappearance of *N. atlantica* (sin.) in the Mediterranean Sea and the North Atlantic up to at least 52°N after ~2.4 Ma (Lourens and Hilgen, 1997; Weaver and Clement, 1987). This suggests the reduction in southward protrusion of colder water masses and hence the *N. atlantica* (sin.) extinction, and a return to a warmer background climate in the Mediterranean region during glacial periods (Lourens, 2008).

The increased AMOC activity is documented by the North Atlantic SST record of Site ODP 982 displaying a plateau starting at ~2.4 Ma indicating more steady climate conditions (Fig. 4A), and a stagnation in Northern Hemisphere ice sheet growth (Bell et al., 2015; Lawrence et al., 2009). Coinciding with this stabilization of North Atlantic SSTs is a cooling in the South Atlantic attributed to a northward piracy of the tropical warmer water pool by a strong AMOC and implying an active interhemispheric climatic seesaw at that time (Fig. 4A, Etourneau et al., 2010; Patterson et al., 2014). Despite the lack of direct data at Site U1389 between the 2.4 to 2.1 Ma interval, seismic records from the Gulf of Cadiz suggest that the hiatus represents a depositional erosion feature caused by intensified bottom current activity, and hence strong MOW flow (Hernandez-Molina et al., 2014b). This would align with the continuous strong AMOC activity in the North Atlantic (Bell et al., 2015).

From the reduction of the  $\delta^{18}\text{O}$  and  $\delta^{13}\text{C}$  gradient between Site U1389 and the MedSea stack (Fig. 4), it appears that after ~2.1 Ma MOW settled and upon Site U1389 (Fig. 4). The reduction in grain-size might also imply more stable MOW behaviour whereas during the transitional phase of the older Interval I MOW was probably more erratic, indicated by the high grain-size variability and the increased  $\delta^{13}\text{C}$  gradient (Fig. 4C and D). Unfortunately, we lack data beyond ~ 2.5 Ma from ODP Sites 549, 552 and 982 to further trace the temporal MOW influence in the high-latitude North Atlantic throughout Interval II but it stands to reason that continued MOW contributions also during Interval II might have contributed to the sustained AMOC activity.

## 5. Conclusions

Based on our results, the supply of MOW to Site U1389 was already established during the Early Pleistocene and not limited to Late and Middle Pleistocene climate conditions. In addition, we find indication that the MOW flow strength might have been modulated by

precession superimposed on glacial-interglacial change, this aligns with findings from the Late Pleistocene at Site U1389, and suggests that Site U1389 is a true recorder of MOW variability also throughout Early Pleistocene. In the broader view of the Early Pleistocene climate evolution we find indication that increased MOW might have contributed to the increased AMOC phases starting from 2.4 Ma, and thus influencing North Atlantic oceanic heat transport.

## Acknowledgements

Firstly, we would like to thank two anonymous reviewers for their careful handling of the manuscript as well as for their constructive comments and suggestions to improve our manuscript. We acknowledge the Integrated Ocean Drilling Program (IODP) for providing the samples used in this study as well as A. van Dijk at Utrecht University for analytical support. This research was funded by NWO-ALW grant (project number 865.10.001) to Lucas J. Lourens and contributions from project P25831-N29 of the Austrian Science Fund (FWF). The data related to this manuscript is publicly available via [www.pangea.de](http://www.pangea.de).

## References

- Ambar, I. and Howe, M. R.: Observations of the mediterranean outflow—II the deep circulation in the vicinity of the gulf of cadiz, *Deep Sea Res. Part A. Oceanogr. Res. Pap.*, 26(5), 555–568, doi:10.1016/0198-0149(79)90096-7, 1979.
- Bahr, A., Jiménez-Espejo, F. J., Kolasinac, N., Grunert, P., Hernández-Molina, F. J., Röhl, U., Voelker, A. H. L., Escutia, C., Stow, D. A. V., Hodell, D. and Alvarez-Zarikian, C. A.: Deciphering bottom current velocity and paleoclimate signals from contourite deposits in the Gulf of Cadiz during the last 140kyr: an inorganic geochemical approach, *Geochemistry, Geophys. Geosystems*, 15(8), 3145–3160, doi:10.1002/2014GC005356, 2014.
- Bahr, A., Kaboth, S., Jiménez-Espejo, F. J., Sierro, F. J., Voelker, A. H. L., Lourens, L., Röhl, U., Reichert, G. J., Escutia, C., Hernández-Molina, F. J., Pross, J. and Friedrich, O.: Persistent monsoonal forcing of Mediterranean Outflow Water dynamics during the late Pleistocene, *Geology*, 43(11), 951–954, doi:10.1130/G37013.1, 2015.
- Baringer, M. O. and Price, J. F.: Mixing and Spreading of the Mediterranean Outflow, *J. Phys. Oceanogr.*, 27, 1654–1677, doi:10.1175/1520-0485(1997)027<1654:MASOTM>2.0.CO;2,

1997.

Becker, J., Lourens, L. J., Hilgen, F. J., van derLaan, E., Kouwenhoven, T. J. and Reichert, G.-J.: Late Pliocene climate variability on Milankovitch to millennial time scales: A high-resolution study of MIS100 from the Mediterranean, *Palaeogeogr. Palaeoclimatol. Palaeoecol.*, 228(3–4), 338–360, doi:10.1016/j.palaeo.2005.06.020, 2005.

Becker, J., Lourens, L. J. and Raymo, M. E.: High-frequency climate linkages between the North Atlantic and the Mediterranean during marine oxygen isotope stage 100 (MIS100), *Paleoceanography*, 21(3), PA3002, doi:10.1029/2005PA001168, 2006.

Bell, D. B., Jung, S. J. A. and Kroon, D.: The Plio-Pleistocene development of Atlantic deep-water circulation and its influence on climate trends, *Quat. Sci. Rev.*, 123, 265–282, doi:10.1016/j.quascirev.2015.06.026, 2015.

Borenäs, K. M., Wåhlin, A. K., Ambar, I. and Serra, N.: The Mediterranean outflow splitting—a comparison between theoretical models and CANIGO data, *Deep Sea Res. Part II Top. Stud. Oceanogr.*, 49, 4195–4205, doi:10.1016/S0967-0645(02)00150-9, 2002.

Bryden, H. L. and Stommel, H. M.: Limiting processes that determine basic features of the circulation in the Mediterranean Sea, *Oceanol. Acta*, 7(3), 289–296, 1984.

Bryden, H. L., Candela, J. and Kinder, T. H.: Exchange through the Strait of Gibraltar, *Prog. Oceanogr.*, 33, 201–248, doi:10.1016/0079-6611(94)90028-0, 1994.

Cramp, A. and O’Sullivan, G.: Neogene sapropels in the Mediterranean: a review, *Mar. Geol.*, 153(1–4), 11–28, doi:10.1016/S0025-3227(98)00092-9, 1999.

Emeis, K.-C., Sakamoto, T., Wehausen, R. and Brumsack, H.-J.: The sapropel record of the eastern Mediterranean Sea — results of Ocean Drilling Program Leg 160, *Palaeogeogr. Palaeoclimatol. Palaeoecol.*, 158(3–4), 371–395, doi:10.1016/S0031-0182(00)00059-6, 2000.

Etourneau, J., Schneider, R., Blanz, T. and Martinez, P.: Intensification of the Walker and Hadley atmospheric circulations during the Pliocene–Pleistocene climate transition, *Earth Planet. Sci. Lett.*, 297(1–2), 103–110, doi:10.1016/j.epsl.2010.06.010, 2010.

Fiúza, A. F. G., Hamann, M., Ambar, I., Díaz del Río, G., González, N. and Cabanas, J. M.: Water masses and their circulation off western Iberia during May 1993, *Deep Sea Res. Part I Oceanogr. Res. Pap.*, 45(7), 1127–1160, doi:10.1016/S0967-0637(98)00008-9, 1998.

474 García-Gallardo, Á., Grunert, P., Van derSchree, M., Sierro, F. J., Jiménez-Espejo, F. J.,  
 475 Alvarez Zarikian, C. A. and Piller, W. E.: Benthic foraminifera-based reconstruction of the first  
 476 Mediterranean-Atlantic exchange in the early Pliocene Gulf of Cadiz, *Palaeogeogr.*  
 477 *Palaeoclimatol. Palaeoecol.*, 472, 93–107, doi:10.1016/j.palaeo.2017.02.009, 2017.

478 Gouhier, T. C., Grinstead, A. and Simko, V.: biwavelet: Conduct univariate and bivariate  
 479 wavelet analyses (Version 0.20.10). [online] Available from:  
 480 <http://github.com/tgouhier/biwavelet>, 2016.

481 Gradstein, F. M., Ogg, J. G. and Hilgen, F. J.: On The Geologic Time Scale, *Newsletters*  
 482 *Stratigr.*, 45(2), 171–188, doi:10.1127/0078-0421/2012/0020, 2012.

483 Grinsted, A., Moore, J. C. and Jevrejeva, S.: Application of the cross wavelet transform and  
 484 wavelet coherence to geophysical time series, *Nonlinear Process. Geophys.*, 11(5/6), 561–566,  
 485 doi:10.5194/npg-11-561-2004, 2004.

486 Grunert, P., Balestra, B., Richter, C., Flores, J.-A., Auer, G., Garcia Gallardo, A. and Piller, W.  
 487 E.: Revised and refined age model for the upper Pliocene of IODP Site U1389 (IODP Exp.  
 488 339, Gulf of Cadiz), *Newsl. Stratigr.*, doi:10.1127/nos/2017/0396, 2017.

489 Hernandez-Molina, F. J., Llave, E., Preu, B., Ercilla, G., Fontan, A., Bruno, M., Serra, N.,  
 490 Gomiz, J. J., Brackenridge, R. E., Sierro, F. J., Stow, D. A.V., Garcia, M., Juan, C., Sandoval,  
 491 N. and Arnaiz, A.: Contourite processes associated with the Mediterranean Outflow Water after  
 492 its exit from the Strait of Gibraltar: Global and conceptual implications, *Geology*, 42(3), 227–  
 493 230, doi:10.1130/G35083.1, 2014a.

494 Hernandez-Molina, F. J., Stow, D. A.V., Alvarez-Zarikian, C. A., Acton, G., Bahr, A., Balestra,  
 495 B., Ducassou, E., Flood, R., Flores, J.-A., Furota, S., Grunert, P., Hodell, D., Jimenez-Espejo,  
 496 F., Kim, J. K., Krissek, L., Kuroda, J., Li, B., Llave, E., Lofi, J., Lourens, L., Miller, M.,  
 497 Nanayama, F., Nishida, N., Richter, C., Roque, C., Pereira, H., Sanchez Goni, M. F., Sierro, F.  
 498 J., Singh, A. D., Sloss, C., Takashimizu, Y., Tzanova, A., Voelker, A., Williams, T. and Xuan,  
 499 C.: Onset of Mediterranean outflow into the North Atlantic, *Science* (80-. ), 344(6189), 1244–  
 500 1250, doi:10.1126/science.1251306, 2014b.

501 Hernández-Molina, F. J., Llave, E., Stow, D. A. V., García, M., Somoza, L., Vázquez, J. T.,  
 502 Lobo, F. J., Maestro, A., Díaz del Río, V., León, R., Medialdea, T. and Gardner, J.: The  
 503 contourite depositional system of the Gulf of Cádiz: A sedimentary model related to the bottom  
 504 current activity of the Mediterranean outflow water and its interaction with the continental



margin, *Deep Sea Res. Part II Top. Stud. Oceanogr.*, 53(11–13), 1420–1463,  
doi:10.1016/j.dsr2.2006.04.016, 2006.

Hernández-Molina, F. J., Stow, D., Alvarez-Zarikian, C., Acton, G., Bahr, A., Balestra, B.,  
Ducassou, E., Flood, R., Flores, J. A., Furota, S., Grunert, P., Hodell, D., Jimenez-Espejo, F.,  
Kim, J. K., Krissek, L., Kuroda, J., Li, B., Llave, E., Lofi, J., Lourens, L., Miller, M., Nanayama,  
F., Nishida, N., Richter, C., Roque, C., Pereira, H., Goñi Fernanda Sanchez, M., Sierro, F. J.,  
Singh, A. D., Sloss, C., Takashimizu, Y., Tzanova, A., Voelker, A., Williams, T. and Xuan, C.:  
IODP Expedition 339 in the Gulf of Cadiz and off West Iberia: Decoding the environmental  
significance of the Mediterranean outflow water and its global influence, *Sci. Drill.*, 16, 1–11,  
doi:10.5194/sd-16-1-2013, 2013.

Hernández-Molina, F. J., Sierro, F. J., Llave, E., Roque, C., Stow, D. A.V, Williams, T., Lofi,  
J., Van derSchee, M., Arnaiz, A., Ledesma, S., Rosales, C., Rodriguez-Tovar, F. J., Pardo-  
Iguzquiza, E. and Brackenridge, R. E.: Evolution of the Gulf of Cadiz margin and southwest  
Portugal contourite depositional system: Tectonic, sedimentary and paleoceanographic  
implications from IODP expedition 339, *Mar. Geol.*, 377, 7–39,  
doi:10.1016/j.margeo.2015.09.013, 2015.

Kaboth, S., Bahr, A., Reichert, G.-J., Jacobs, B. and Lourens, L. J.: New insights into upper  
MOW variability over the last 150kyr from IODP 339 Site U1386 in the Gulf of Cadiz, *Mar.*  
*Geol.*, 377, 136–145, doi:10.1016/j.margeo.2015.08.014, 2016.

Kaboth, S., deBoer, B., Bahr, A., Zeeden, C. and Lourens, L. J.: Mediterranean Outflow Water  
dynamics during the past ~570 kyr: Regional and Global implications: Mid- to Late Pleistocene  
MOW, *Paleoceanography*, doi:10.1002/2016PA003063, 2017.

Khelifi, N., Sarnthein, M., Andersen, N., Blanz, T., Frank, M., Garbe-Schonberg, D., Haley, B.  
A., Stumpf, R. and Weinelt, M.: A major and long-term Pliocene intensification of the  
Mediterranean outflow, 3.5–3.3 Ma ago, *Geology*, 37(9), 811–814, doi:10.1130/G30058A.1,  
2009.

Khelifi, N. and Frank, M.: A major change in North Atlantic deep water circulation 1.6 million  
years ago, *Clim. Past*, 10(4), 1441–1451, doi:10.5194/cp-10-1441-2014, 2014.

Khelifi, N., Sarnthein, M., Frank, M., Andersen, N. and Garbe-Schönberg, D.: Late Pliocene  
variations of the Mediterranean outflow, *Mar. Geol.*, 357, 182–194,  
doi:10.1016/j.margeo.2014.07.006, 2014.

536 Lang, D. C., Bailey, I., Wilson, P. A., Chalk, T. B., Foster, G. L. and Gutjahr, M.: Incursions  
 537 of southern-sourced water into the deep North Atlantic during late Pliocene  
 538 glacial?intensification, *Nat. Geosci.*, 9(5), 375–379, doi:10.1038/ngeo2688, 2016.

539 Lawrence, K. T., Herbert, T. D., Brown, C. M., Raymo, M. E. and Haywood, A. M.: High-  
 540 amplitude variations in North Atlantic sea surface temperature during the early Pliocene warm  
 541 period, *Paleoceanography*, 24(2), PA2218, doi:10.1029/2008PA001669, 2009.

542 Lisiecki, L. E.: Atlantic overturning responses to obliquity and precession over the last 3 Myr,  
 543 *Paleoceanography*, 29(2), 71–86, doi:10.1002/2013PA002505, 2014.

544 Liu, Y., San Liang, X. and Weisberg, R. H.: Rectification of the Bias in the Wavelet Power  
 545 Spectrum, *J. Atmos. Ocean. Technol.*, 24(12), 2093–2102, doi:10.1175/2007JTECHO511.1,  
 546 2007.

547 Llave, E., Schönfeld, J., Hernández-Molina, F. J., Mulder, T., Somoza, L., Díaz Del Río, V.  
 548 and Sánchez-Almazo, I.: High-resolution stratigraphy of the Mediterranean outflow contourite  
 549 system in the Gulf of Cadiz during the late Pleistocene: The impact of Heinrich events, *Mar.*  
 550 *Geol.*, 227, 241–262, doi:10.1016/j.margeo.2005.11.015, 2006.

551 Lofi, J., Voelker, A. H. L., Ducassou, E., Hernández-Molina, F. J., Sierro, F. J., Bahr, A.,  
 552 Galvani, A., Lourens, L. J., Pardo-Igúzquiza, E., Pezard, P., Rodríguez-Tovar, F. J. and  
 553 Williams, T.: Quaternary chronostratigraphic framework and sedimentary processes for the  
 554 Gulf of Cadiz and Portuguese Contourite Depositional Systems derived from Natural Gamma  
 555 Ray records, *Mar. Geol.*, doi:10.1016/j.margeo.2015.12.005, 2015.

556 Loubere, P.: Changes in mid-depth North Atlantic and Mediterranean circulation during the  
 557 Late Pliocene — Isotopic and sedimentological evidence, *Mar. Geol.*, 77(1–2), 15–38,  
 558 doi:10.1016/0025-3227(87)90081-8, 1987.

559 Lourens, L. J.: Revised tuning of Ocean Drilling Program Site 964 and KC01B (Mediterranean)  
 560 and implications for the  $\delta^{18}\text{O}$ , tephra, calcareous nannofossil, and geomagnetic reversal  
 561 chronologies of the past 1.1 Myr, *Paleoceanography*, 19(3), PA3010,  
 562 doi:10.1029/2003PA000997, 2004.

563 Lourens, L. J.: On the Neogene-Quaternary debate, *Episodes*, 31, 239–242, 2008.

564 Lourens, L. J. and Hilgen, F. J.: Long-periodic variations in the earth's obliquity and their  
 565 relation to third-order eustatic cycles and late Neogene glaciations, *Quat. Int.*, 40, 43–52,

doi:10.1016/S1040-6182(96)00060-2, 1997.

Lourens, L. J., Hilgen, F. J., Gudjonsson, L. and Zachariasse, W. J.: Late Pliocene to early Pleistocene astronomically forced sea surface productivity and temperature variations in the Mediterranean, *Mar. Micropaleontol.*, 19(1–2), 49–78, doi:10.1016/0377-8398(92)90021-B, 1992.

Lourens, L. J., Hilgen, F. J., Raffi, I. and Vergnaud-Grazzini, C.: Early Pleistocene chronology of the Vrica Section (Calabria, Italy), *Paleoceanography*, 11(6), 797–812, doi:10.1029/96PA02691, 1996a.

Lourens, L. J., Antonarakou, A., Hilgen, F. J., VanHoof, A. A. M., Vergnaud-Grazzini, C. and Zachariasse, W. J.: Evaluation of the Plio-Pleistocene astronomical timescale, *Paleoceanography*, 11(4), 391–413, doi:10.1029/96PA01125, 1996b.

Marchitto, T. M., Curry, W. B., Lynch-Stieglitz, J., Bryan, S. P., Cobb, K. M. and Lund, D. C.: Improved oxygen isotope temperature calibrations for cosmopolitan benthic foraminifera, *Geochim. Cosmochim. Acta*, 130, 1–11, doi:10.1016/j.gca.2013.12.034, 2014.

Martinez-Garcia, A., Rosell-Mele, A., McClymont, E. L., Gersonde, R. and Haug, G. H.: Subpolar Link to the Emergence of the Modern Equatorial Pacific Cold Tongue, *Science* (80-. ), 328(5985), 1550–1553, doi:10.1126/science.1184480, 2010.

Millot, C.: Another description of the Mediterranean Sea outflow, *Prog. Oceanogr.*, 82, 101–124, doi:10.1016/j.pocean.2009.04.016, 2009.

Millot, C.: Heterogeneities of in- and out-flows in the Mediterranean Sea, *Prog. Oceanogr.*, 120, 254–278, doi:10.1016/j.pocean.2013.09.007, 2014.

Millot, C., Candela, J., Fuda, J.-L. and Tber, Y.: Large warming and salinification of the Mediterranean outflow due to changes in its composition, *Deep Sea Res. Part I Oceanogr. Res. Pap.*, 53(4), 656–666, doi:10.1016/j.dsr.2005.12.017, 2006.

Mulder, T., Lecroart, P., Hanquiez, V., Marches, E., Gonthier, E., Guedes, J.-C., Thiébot, E., Jaaidi, B., Kenyon, N., Voisset, M., Perez, C., Sayago, M., Fuchey, Y. and Bujan, S.: The western part of the Gulf of Cadiz: contour currents and turbidity currents interactions, *Geo-Marine Lett.*, 26(1), 31–41, doi:10.1007/s00367-005-0013-z, 2006.

Myers, P. G.: Flux-forced simulations of the paleocirculation of the Mediterranean, *Paleoceanography*, 17(1), 1009, doi:10.1029/2000PA000613, 2002.

596 Patterson, M. O., McKay, R., Naish, T., Escutia, C., Jimenez-Espejo, F. J., Raymo, M. E.,  
 597 Meyers, S. R., Tauxe, L., Brinkhuis, H., Klaus, A., Fehr, A., Bendle, J. A. P., Bijl, P. K., Bohaty,  
 598 S. M., Carr, S. A., Dunbar, R. B., Flores, J. A., Gonzalez, J. J., Hayden, T. G., Iwai, M., Katsuki,  
 599 K., Kong, G. S., Nakai, M., Olney, M. P., Passchier, S., Pekar, S. F., Pross, J., Riesselman, C.  
 600 R., Röhl, U., Sakai, T., Shrivastava, P. K., Stickley, C. E., Sugasaki, S., Tuo, S., van deFlierdt,  
 601 T., Welsh, K., Williams, T. and Yamane, M.: Orbital forcing of the East Antarctic ice sheet  
 602 during the Pliocene and Early Pleistocene, *Nat. Geosci.*, 7(11), 841–847,  
 603 doi:10.1038/ngeo2273, 2014.

604 Peliz, A., Marchesiello, P., Santos, A. M. P., Dubert, J., Teles-Machado, A., Marta-Almeida,  
 605 M. and LeCann, B.: Surface circulation in the Gulf of Cadiz: 2. Inflow-outflow coupling and  
 606 the Gulf of Cadiz slope current, *J. Geophys. Res.*, 114(C3), doi:10.1029/2008JC004771, 2009.

607 Peliz, Á., Dubert, J., Santos, A. M. P., Oliveira, P. B. and LeCann, B.: Winter upper ocean  
 608 circulation in the Western Iberian Basin—Fronts, Eddies and Poleward Flows: an overview,  
 609 *Deep Sea Res. Part I Oceanogr. Res. Pap.*, 52(4), 621–646, doi:10.1016/j.dsr.2004.11.005,  
 610 2005.

611 R Core Team: R: A language and environment for statistical computing, [online] Available  
 612 from: <http://www.r-project.org/>, 2014.

613 Raffi, I., Backman, J., Fornaciari, E., Pälike, H., Rio, D., Lourens, L. and Hilgen, F.: A review  
 614 of calcareous nannofossil astrobiochronology encompassing the past 25 million years☆, *Quat.*  
 615 *Sci. Rev.*, 25(23–24), 3113–3137, doi:10.1016/j.quascirev.2006.07.007, 2006.

616 Raymo, M. E., Hodell, D. and Jansen, E.: Response of deep ocean circulation to initiation of  
 617 northern hemisphere glaciation (3-2 MA), *Paleoceanography*, 7(5), 645–672,  
 618 doi:10.1029/92PA01609, 1992.

619 Rogerson, M., Rohling, E. J., Weaver, P. P. E. and Murray, J. W.: Glacial to interglacial  
 620 changes in the settling depth of the Mediterranean Outflow plume, *Paleoceanography*, 20(3),  
 621 1–12, doi:10.1029/2004PA001106, 2005.

622 Rogerson, M., Rohling, E. J. and Weaver, P. P. E.: Promotion of meridional overturning by  
 623 Mediterranean-derived salt during the last deglaciation, *Paleoceanography*, 21(4), PA4101,  
 624 doi:10.1029/2006PA001306, 2006.

625 Rogerson, M., Schönfeld, J. and Leng, M. J.: Qualitative and quantitative approaches in

626 palaeohydrography: A case study from core-top parameters in the Gulf of Cadiz, *Mar. Geol.*,  
627 280(1–4), 150–167, doi:10.1016/j.margeo.2010.12.008, 2011.

628 Rohling, E. J., Marino, G. and Grant, K. M.: Mediterranean climate and oceanography, and the  
629 periodic development of anoxic events (sapropels), *Earth-Science Rev.*, 143, 62–97,  
630 doi:10.1016/j.earscirev.2015.01.008, 2015.

631 Rossignol-Strick, M.: African monsoons, an immediate climate response to orbital insolation,  
632 *Nature*, 304(5921), 46–49, doi:10.1038/304046a0, 1983.

633 Rossignol-Strick, M.: Mediterranean Quaternary sapropels, an immediate response of the  
634 African monsoon to variation of insolation, *Palaeogeogr. Palaeoclimatol. Palaeoecol.*, 49(3–4),  
635 237–263, doi:10.1016/0031-0182(85)90056-2, 1985.

636 Rutherford, S. and D’Hondt, S.: Early onset and tropical forcing of 100,000-year Pleistocene  
637 glacial cycles, *Nature*, 408(6808), 72–75, doi:10.1038/35040533, 2000.

638 Schönfeld, J.: A new benthic foraminiferal proxy for near-bottom current velocities in the Gulf  
639 of Cadiz, northeastern Atlantic Ocean, *Deep. Res. Part I Oceanogr. Res. Pap.*, 49, 1853–1875,  
640 doi:10.1016/S0967-0637(02)00088-2, 2002.

641 Schönfeld, J. and Zahn, R.: Late Glacial to Holocene history of the Mediterranean outflow.  
642 Evidence from benthic foraminiferal assemblages and stable isotopes at the Portuguese margin,  
643 *Palaeogeogr. Palaeoclimatol. Palaeoecol.*, 159, 85–111, doi:10.1016/S0031-0182(00)00035-3,  
644 2000.

645 Schulz, M. and Mudelsee, M.: REDFIT: estimating red-noise spectra directly from unevenly  
646 spaced paleoclimatic time series, *Comput. Geosci.*, 28(28), 421–426, 2002.

647 Shackleton, N. J. and Hall, M. A.: Oxygen and carbon isotope stratigraphy of the deep sea  
648 drilling project hole 552A: Plio-Pleistocene glacial history, *Initial Reports DSDP*, 81, 599–609.  
649 doi:10.1029/2000PA000513, 1984.

650 Stow, D. A.V., Hernández-Molina, F. J. and Alvarez-Zarikian, C.: Expedition 339 Summary,  
651 edited by Expedition 339 Scientists, *Exped. 339 Summ., Proceeding(339)*,  
652 doi:10.2204/iodp.proc.339.104.2013, 2013.

653 Torrence, C. and Compo, G. P.: A Practical Guide to Wavelet Analysis, *Bull. Am. Meteorol.*  
654 *Soc.*, 79(1), 61–78, doi:10.1175/1520-0477(1998)079<0061:APGTWA>2.0.CO;2, 1998.

655 Toucanne, S., Mulder, T., Schönfeld, J., Hanquiez, V., Gonthier, E., Duprat, J., Cremer, M.  
 656 and Zaragosi, S.: Contourites of the Gulf of Cadiz: A high-resolution record of the  
 657 paleocirculation of the Mediterranean outflow water during the last 50,000 years, *Palaeogeogr.*  
 658 *Palaeoclimatol. Palaeoecol.*, 246, 354–366, doi:10.1016/j.palaeo.2006.10.007, 2007.

659 Verhallen, P. J.: Late Pliocene to Early Pleistocene Mediterranean mud-dwelling foraminifera:  
 660 influence of a changing environment on community structure and evolution., 1991.

661 Voelker, A., Lebreiro, S., Schonfeld, J., Cacho, I., Erlenkeuser, H. and Abrantes, F.:  
 662 Mediterranean outflow strengthening during northern hemisphere coolings: A salt source for  
 663 the glacial Atlantic?, *Earth Planet. Sci. Lett.*, 245(1–2), 39–55, doi:10.1016/j.epsl.2006.03.014,  
 664 2006.

665 Voelker, A. H. L., Colman, A., Olack, G., Waniek, J. J. and Hodell, D.: Oxygen and hydrogen  
 666 isotope signatures of Northeast Atlantic water masses, *Deep Sea Res. Part II Top. Stud.*  
 667 *Oceanogr.*, 116, 89–106, doi:10.1016/j.dsr2.2014.11.006, 2015.

668 Weaver, P.P.E and Clement, B.M.: Magnetobiostratigraphy of planktonic foraminiferal datums:  
 669 Deep Sea Drilling Project Leg 94, North Atlantic, vol. 94, U.S. Government Printing Office.  
 670 1987.

671 deWinter, N. J., Zeeden, C. and Hilgen, F. J.: Low-latitude climate variability in the Heinrich  
 672 frequency band of the Late Cretaceous greenhouse world, *Clim. Past*, 10(3), 1001–1015,  
 673 doi:10.5194/cp-10-1001-2014, 2014.

674 Zachariasse, W. J., Gudjonsson, L., Hilgen, F. J., Langereis, C. G., Lourens, L. J., Verhallen,  
 675 P. J. J. M. and Zijderveld, J. D. A.: Late Gauss to Early Matuyama invasions of  
 676 *Neogloboquadrina Atlantica* in the Mediterranean and associated record of climatic change,  
 677 *Paleoceanography*, 5(2), 239–252, doi:10.1029/PA005i002p00239, 1990.

678 Zahn, R., Sarnthein, M. and Erlenkeuser, H.: Benthic isotope evidence for changes of the  
 679 Mediterranean outflow during the Late Quaternary, *Paleoceanography*, 2(6), 543–559,  
 680 doi:10.1029/PA002i006p00543, 1987.

681 Zijderveld, J. D. A., Hilgen, F. J., Langereis, C. G., Verhallen, P. and Zachariasse, W. J.:  
 682 Integrated magnetostratigraphy and biostratigraphy of the upper Pliocene-lower Pleistocene  
 683 from the Monte Singa and Crotone areas in Calabria, Italy, *Earth Planet. Sci. Lett.*, 107(3–4),  
 684 697–714, 1991.

## Figure Captions

Figure 1: (A) Study area with illustration of modern MOW pathways modified after (Bahr et al. 2015). Site location of U1389 (yellow dot) is marked. (B) Overview map of the Mediterranean Sea. Location of the Singa and Vrica sections in Italy (yellow dot) are marked. Black square indicates Gulf of Cadiz study area. (C) Water mass circulation in the Mediterranean Sea (modified after Cramp and O'Sullivan, 1999). MAW = Mixed Atlantic surface water; LIW = Levantine intermediate water; EMDW = Eastern Mediterranean deep water; WMDW = Western Mediterranean deep water (D) CTD depth profile of temperature (red line) and salinity (blue line) at Site U1389 derived from the World Ocean Database 2013. The data points of  $\delta^{18}\text{O}_{\text{water}}$  (black line) are derived from neighbouring EUROFLEETS-Iberian-Forams Cruise site IB-F9 (36° 48.40' N; 7° 42.85' W) (Voelker et al., 2015). NACW<sub>st</sub>=North Atlantic Central water of subtropical origin; NACW<sub>sp</sub>= North Atlantic water of subpolar origin; MOW=Mediterranean Outflow water.

Figure 2: The  $\delta^{18}\text{O}$  (A) and  $\delta^{13}\text{C}$  (B) interspecies correlation between benthic foraminifera *Cibicides ungerianus* and *Planulina ariminensis* at Site U1389. Parallel measurements were conducted throughout both investigated intervals. Linear square regression (black line) equation and Pearson correlation coefficient ( $R^2$ ) are shown.

Figure 3: Chronology of Site U1389. Assigned marine isotope stages (MIS) follow Lourens et al. (2004). (A) Both intervals of the  $\delta^{18}\text{O}$  record of Site U1389 on shipboard mbsf scale correlated to the benthic  $\delta^{18}\text{O}$  record of the Mediterranean Sea (MedSea stack) after Lourens et al. (1996a, unpublished data). Chronostratigraphy of MedSea stack is based on tuning sapropel midpoints to La2004 65° N summer insolation (Lourens, 2004). Lines with arrows indicate selected tie points used for the age model (a full list of tie points is available in Table 2). Black triangles with numbers indicating used biostratigraphic and paleomagnetic tie points as referenced in Table 1. Black and white bar at the top represents core recovery following Hernández-Molina et al. (2013) (B) Comparison of the benthic  $\delta^{18}\text{O}$  record of Site U1389 on new time scale according to our tuning, and the benthic  $\delta^{18}\text{O}$  MedSea stack on its respective age model (Lourens et al. 2004) (C) Calculated sedimentation rates for Site U1389.

Figure 4: (A) UK<sup>37</sup> based sea-surface temperature (SST) record of North Atlantic Site ODP 982 (Lawrence et al., 2009) and South Atlantic Site ODP 1090 (Martinez-Garcia et al., 2010). The running mean has a band width of 23. AMOC phases are marked by black arrows and follow the chronology of Bell et al. (2015). (B) Benthic  $\delta^{18}\text{O}$  records of both investigated

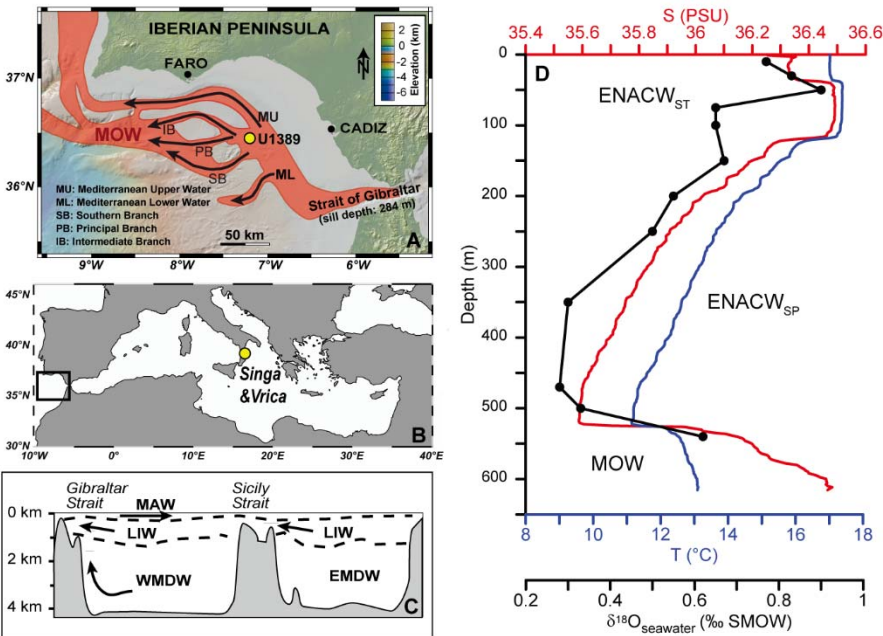
intervals at Site U1389. Interval I comprises the time frame of 2.6 to 2.4 Ma and Interval II 2.1 to 1.8 Ma. Isotopic gradient between both records is indicated by the grey-shaded area. (C) Comparison of  $\delta^{13}\text{C}$  of *P. ariminensis* for both investigated intervals at Site U1389 and  $\delta^{13}\text{C}$  of the MedSea stack (Lourens et al. 1996a, unpublished data). The running means have a band width of 5. The *C. ungerianus* based  $\delta^{13}\text{C}$  values of the MedSea stack were adjusted to *P. ariminensis*  $\delta^{13}\text{C}$  values of Site U1389 following the interspecies correction presented in this study (D) Grain-size (63-150  $\mu\text{m}$  wt.-%) records for both investigated intervals at Site U1389. The filtered  $\sim 23$  kyr signal ( $f = 0.05 \pm 0.01$ ) of the grain-size signal is indicated by the black dotted-line. Sapropel mid-points are marked by orange arrows and follow the chronology of Emeis et al. (2000).

Figure 5: REDFIT power spectra of the grain-size values (63-150 $\mu\text{m}$  fraction in wt.-%) for both investigated intervals of Site U1389: (A) Interval I = 2.6-2.4 Ma and (B) Interval II: 2.1-1.8 Ma). The 90% (red), 80% (blue) and AR1 red noise (black) confidence levels are given. (C) Wavelet analysis of the grain-size values (63-150 $\mu\text{m}$  fraction in wt.-%) during Interval I and (D) Wavelet analysis of the grain-size values (63-150 $\mu\text{m}$  fraction in wt.-%) during Interval II. Cone of confidence (white) for both Intervals is marked. Areas with >95% significance level are marked by black lines. Periods corresponding to (semi, 1/3)-precession are marked with dashed white lines.



735 **Figure 1**

736



737

**Figure 2**

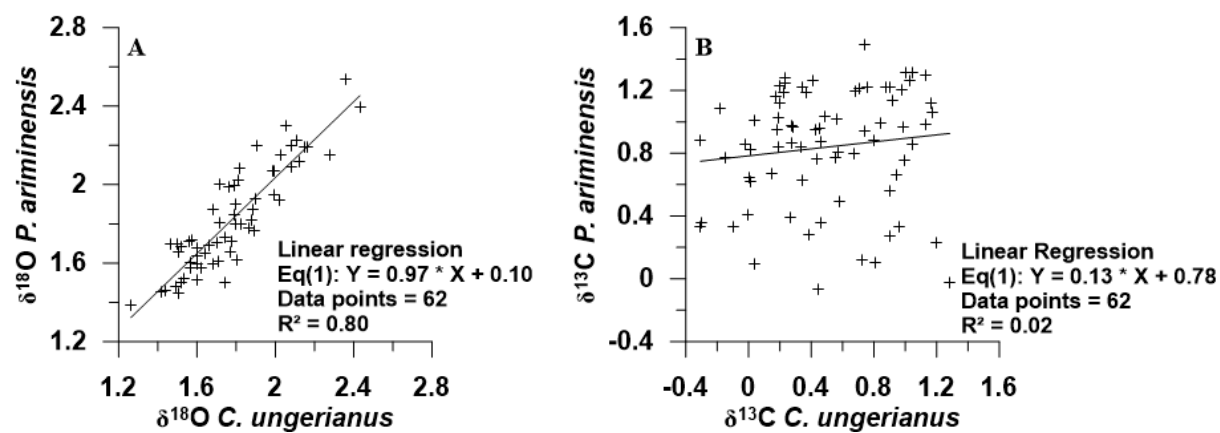


**Figure 3**

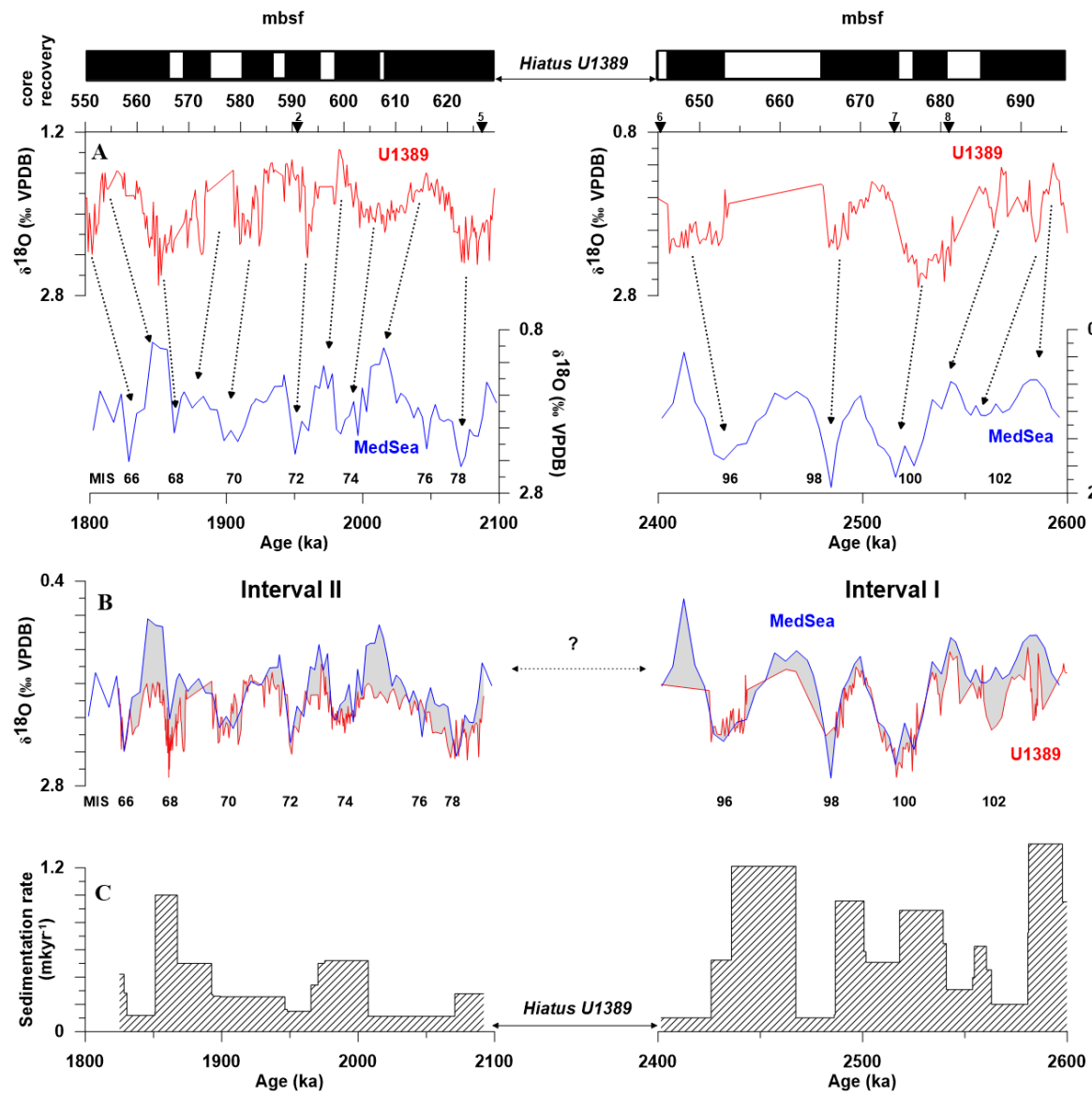
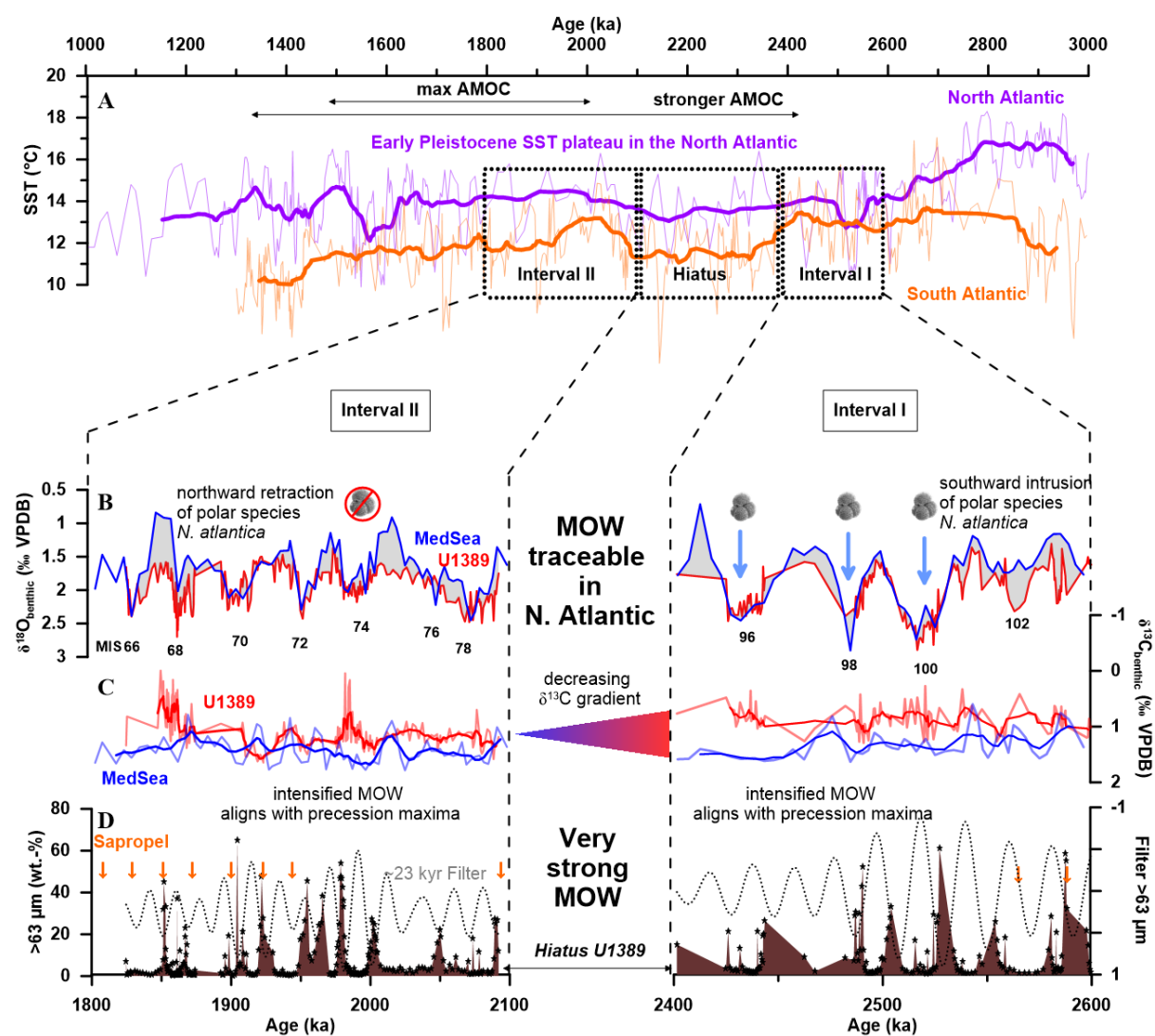
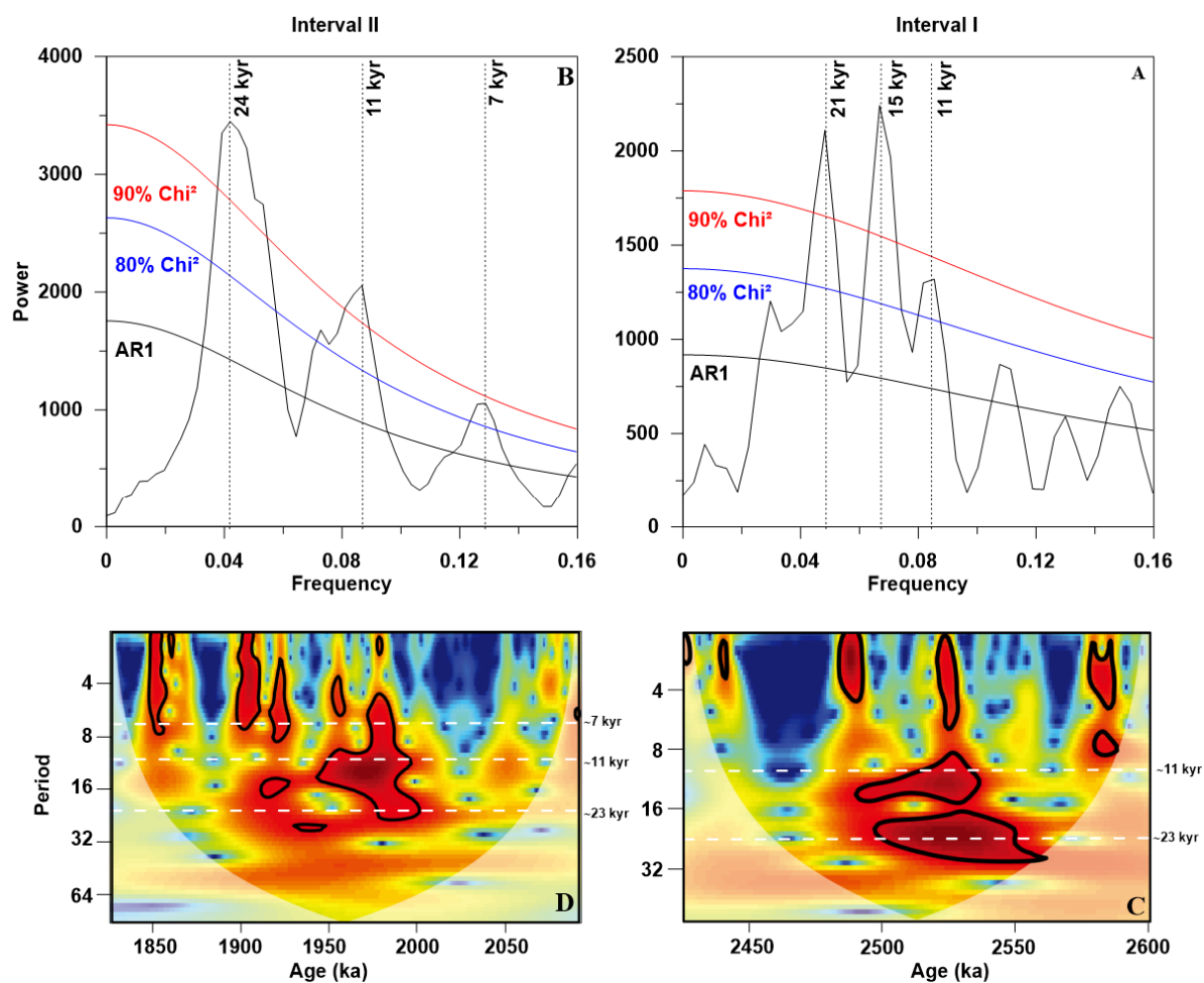


**Figure 4**



748 **Figure 5**

749



750

751

752 **Table Captions**

753 Table 1: Paleomagnetic and biostratigraphic tie points used in the primary age model of Site  
754 U1389 based on shipboard data following Hernández-Molina et al. (2013) and Stow et al.  
755 (2013). 1 = Gradstein et al. (2012); 2 = Raffi et al. (2006); 3= Lourens et al. (2004); 4 = (Grunert  
756 et al., 2017)

757 Table 2: Paleomagnetic and biostratigraphic tie points used in the primary age model of Site  
758 U1389 based on shipboard data following Hernández-Molina et al. (2013) and Stow et al.  
759 (2013). 1 = Gradstein et al. (2012); 2 = Raffi et al. (2006); 3= Lourens et al. (2004); 4 = Grunert  
760 et al. 2017

761 **Table 1**

No.	Event	TOP Depth (mbsf)	BOT Depth (mbsf)	Age (ka)	Ref.
1	Top Olduvai	542.00		1806	1
2	Bottom Olduvai		592.00	1945	1
3	Matuyama/Gauss	699.00		2581	4
4	LO <i>Calcidiscus macintyrie</i>	510.99	515.65	1660	2
5	FO <i>Globorotalia inflata</i>	627.21	630.21	2090	3
6	LO <i>Globorotalia puncticulata</i>	645.02	646.61	2410	3
7	LO <i>Discoaster pentradiatus</i>	674.25	681.98	2500	2
8	LO <i>Discoaster scurlus</i>	681.98	693.70	2530	2
9	LO <i>Discoaster tamalis</i>	799.75	800	2800-2830	4

762

<b>Depth (mbsf)</b>	<b>Age (ka)</b>
512	1660
542	1806
551.25	1828
554	1851
564	1861
570	1867
574	1875
580	1898
592	1945
595	1965
600	1975
615.63	2005
623	2070
629.1	2092
629.75	2117.5
631.1	2132.5
646	2425
648.75	2435.5
665.1	2462.5
666.3	2486
673	2500
677.45	2517.5
687	2539
689	2552
691.5	2560
693.5	2583
699	2581
799.75	2800